Energy Advances

Accepted Manuscript

This article can be cited before page numbers have been issued, to do this please use: U. Mani, *Energy Adv.*, 2024, DOI: 10.1039/D4YA00358F.

ROYAL SOCIETY OF CHEMISTRY

rsc.li/energy-advances

View Article Online
DOI: 10.1039/D4YA00358F

Zinc-Iron (Zn-Fe) Redox Flow Battery Single to Stack Cells: A Futuristics Solution for High Energy Storage Off-Grid Applications

Mani Ulaganathan[a, b*]

[a]Department of Physics, Amrita School of Physical Sciences Coimbatore, Amrita Vishwa Vidyapeetham Coimbatore, India-641 112

[b]Functional Materials Laboratory, Amrita School of Engineering Coimbatore, Amrita Vishwa Vidyapeetham, India-641 112

Abstract

The decoupling nature of energy and power of redox flow batteries make them an efficient energy storage solution for sustainable off-grid applications. Recently, aqueous zinc-iron redox flow batteries have received great interest due to their eco-friendliness, cost-effectiveness, non-toxicity, and abundance. However, the development of zinc-iron redox flow batteries (RFBs) remains challenging due to severe inherent difficulties such as zinc dendrites, iron (III) hydrolysis, ion-crossover, hydrogen evolution reactions (HER), and expensive membranes which hinder commercialization. Many scientific initiatives have been commenced in the past few years to address these primary difficulties, paving the way for high-performance zinc-iron (Zn-Fe) RFBs. This review collectively provides the various aspects of the Zn-Fe RFB including basic electrochemical cell chemistry of anolyte, catholyte, different approaches made on electrodes, electrolytes, membranes, and other cell components to overcome the above issues. This overview accomplishes with the perceptions into future advances and viewpoints for obtaining the high-performance Zn-Fe RFBs.

Keywords: Redox Flow Batteries, Zinc -Iron, Aqueous Flow Batteries, Energy density, Power density.

Corresponding Author: m_ulaganathan@cb.amrita.edu & nathanphysics@gmail.com (M. Ulaganathan)

View Article Online
DOI: 10.1039/D4YA00358F

1. Introduction

Rapid population expansion intensifies the effects of climate change by draining resources and also exposes more individuals to climate-related hazards. This scenario has to be alleviated by reducing and preventing greenhouse gas emissions into the atmosphere. In this regard, energy storage has been highlighted as a significant factor in climate change mitigation. Globally, only 3% of available electricity capacity is stored. To keep global warming under 2°C, energy storage capacity must be increased three-fold by 2050[1]. To do this, we must consider inventive approaches to accelerate the development of energy storage technologies. Electrochemical energy storage systems (ESS) are the most attractive technologies for storing electricity and can be used when supply is insufficient to satisfy the demand[2-4]. In the future, intermittent renewable resources such as wind and solar are expected to provide a greater share of electrical energy hence making these devices crucial for developing clean and cost-effective solutions.

Redox flow batteries (RFBs) have received much interest because of their appealing decoupling power and energy density features, making them more suitable for large-scale energy storage applications[5-7]. This feature is more advantageous over other conventional batteries such as Li-ion, lead acid batteries, etc., In general, RFBs are a hybrid form of batteries and fuel cells; they can store electrical energy and release it when it mandates. In RFBs, energy is stored in the electrolytes containing different redox active species that can undergo redox reactions at the electrodes[8-11]. A typical RFB cell configuration consists of anode and cathode compartments separated by an ion exchange membrane (IEM) or separator. The electrolytes are stored externally in a separate tank which is circulated into the respective cell compartment with the help of a pump. An ion-exchange membrane allows selective ions (such as H^+, Cl^-,

View Article Online
DOI: 10.1039/D4YA00358F

etc.,) between the compartments to maintain electrical neutrality during battery operations by preventing redox active species crossover. As mentioned before, the most distinguishing feature of RFBs is their ability to decouple power and energy density; the power density can be enhanced by increasing the number of cells as well as by increasing the active area of the electrode; the energy density can be augmented by increasing the volume or concentration of electrolyte. The energy density of RFBs is determined using the below equation[12].

$$E = n.\ C.\ F.\ \Delta V \ \ldots\ldots\ldots (1)$$

Where n – is the number of moles of electrons involved in the redox reactions, C – is the concentration of redox-active species, F – is Faraday's constant (95485 C mol^{-1}), and ΔV – is the potential difference between two redox-active species.

All of these parameters are directly linked with the electrolyte characteristics, therefore choosing an appropriate redox couple is of prime importance in RFBs, as it dictates the energy density of RFBs. RFBs can be classified into two different categories such as i) all soluble RFB; and ii) metal hybrid RFB. In all soluble RFBs, the redox couples in both anolyte and catholyte are in the soluble form during cell operations. On the other hand, in the hybrid RFB, the metal ions undergo a phase change from liquid to solid state conversion during the charging process (i.e., reduction at the anode). The metal gets oxidized during the discharge and reaches the electrolyte tank. All vanadium RFB is one of the best examples for all soluble RFBs, where the anolyte and catholyte have soluble redox couples of V^{2+}/V^{3+} and V^{4+}/V^{5+}, respectively[13]. Conversely, Zn^{2+} is converted into Zn^{0} at the anode (reduction) and the oxidation will occur in the positive electrode during the charging process where the redox species are in the soluble form [14-15].

Zinc-based RFBs have an immense attraction for energy storage applications due to their high theoretical capacity (820 mAh/g), two-electron reaction, fast plating/stripping process, low reduction potential (-0.76 V vs SHE in neutral/acidic, -1.26 V vs SHE in alkaline

View Article Online
DOI: 10.1039/D4TA00358F

medium), abundance, and eco-friendliness. So far, various zinc-based RFBs have been reported such as Zn/Ce[16-18], Zn/Br_2[14, 19-20], Zn/V[15, 19, 21-22], Zn/organic couple[23], Zn/Cl_2[24], Zn/I_3-[25], Zn/Fe[26], and Zn/Mn[27-28]. Among these, Zn/Br_2 RFB has the most matured technology and has been largely investigated. However, issues like environmental pollution, bromine's high corrosive nature, and bromine's high vapor pressure severely affect their commercialization. Therefore, the identification of a safe, eco-friendly, and abundant redox couple alternative to bromine redox couple is a very important topic of research at this global scenario. Iron is identified as a better alternative to bromine. It is well known that iron is the most abundant metal and the fourth most abundant of all the elements in the earth's crust. It mainly occurs as oxides such as haematite (Fe_2O_3), magnetite (Fe_3O_4), and iron pyrites (FeS_2). Iron reserves are 560 times those of zinc, yet its price is 1/43 of that of zinc[29].

Recently, Iron-based RFBs have emerged as an interesting candidate for long-term electrochemical storage due to their multivalent nature(Fe, Fe^{2+}, and Fe^{3+}), good reversibility of Fe^{3+}/Fe^{2+} (+0.77 V vs SHE, theoretical capacity of 450 mAh/g) and Fe^{2+}/Fe (-0.44 V vs SHE, theoretical capacity of 960 mAh/g), eco-friendliness, and low elemental cost[30]. The aforementioned features of the iron have been considered to be of substantial interest in the iron-based RFBs[29]. However, the reversibility and the high redox potential of Fe^{2+}/Fe^{3+} redox reaction pave much attention as a catholyte in various RFBs, such as Zn-Fe, Fe-Mn, Fe-S etc[31]. More specifically, the Zn-Fe is attracted largely due to its high cell voltage and high practical energy density at low cost. These benefits make Zn-iron-based RFBs a perfect choice for use in large-scale energy storage for off-grid applications. A schematic representation of the various applications of Zn-Fe RFBs is shown in Figure 1. However, the hydrolysis of F(III), ion crossover, low solubility, and Zn dendrite formations are the major concerns. Figure 2 shows various issues associated with the Zn-Fe RFBs. To overcome this, various approaches

View Article Online
DOI: 10.1039/D4TA00358F

have been made to the Zn-Fe in recent times. Therefore, this review is exclusively focused on the recent developments of Zn-Fe-based RFBs along with their future perspectives.

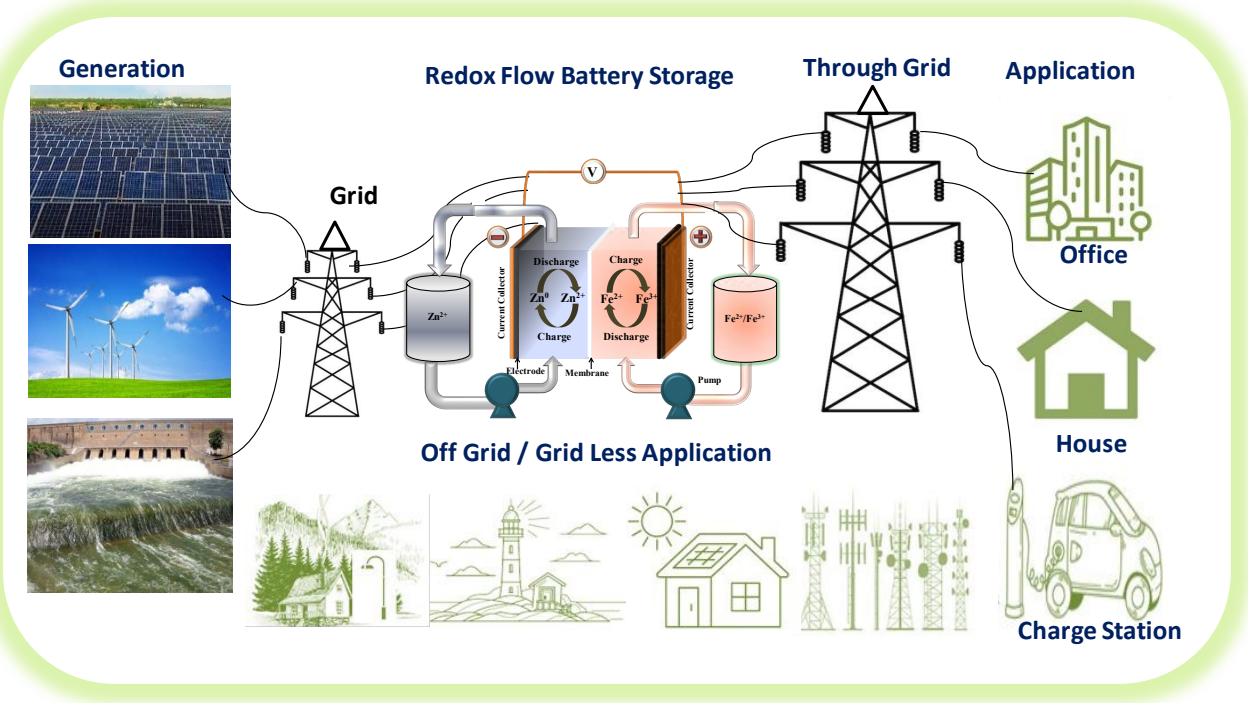

Figure 1: Schematic representation of various applications of the RFBs in both off-grid and through-grid.

2.1 Electrochemistry of zinc redox couple

(a) Alkaline medium:

$$Zn(OH)_4^{2-} + 2e^- \rightleftharpoons Zn + 4OH^- \quad E^\circ = -1.26 \text{ V vs SHE} \ldots\ldots\ldots (2)$$

The precursor zinc oxide (ZnO) is generally prepared by dissolving it in a strong base (NaOH or KOH) to produce zincate anions ($Zn(OH)_4^{2-}$), which are then involved in the redox reaction at the electrode. The conductivity and solubility of zincate anions are always dependent on the pH of the electrolyte. In general, electrodeposition of zinc takes place via mass transfer, pre-transformation, charge transfer, and electro-crystallization.

View Article Online
DOI: 10.1039/D4YA00358F

(b) Neutral/acidic medium:

In the neutral/acidic medium, zinc electrodeposition occurs differently because the electrolyte simply contains zinc ions (Zn^{2+}) rather than zincate ions. The electrodeposition of zinc under neutral/acidic conditions is discussed below.

$$Zn^{2+} + 2e^- \rightleftharpoons Zn \quad E^\circ = -0.76 \text{ V vs SHE} \ldots\ldots\ldots (3)$$

Zinc ions (Zn^{2+}) undergo three stages, similar to alkaline medium, but there is no pre-transformation step since zincate ions are absent in the electrolyte. The Zn^{2+} ions are immediately reduced at the electrode surface, resulting in the nucleation process.

It can be seen that zinc exhibits a very low redox potential of -1.22 V vs SHE in an alkaline medium which would be more beneficial to a battery to achieve high voltage when paired with high redox potential couples[32-33]. Alkaline medium often has better electrolyte conductivity than neutral medium, resulting in a faster transfer of OH^- than K^+ or Na^+. Therefore, alkaline zinc-based RFBs can operate at a high current rate and as a result, high power densities can be achieved.

2.2. Electrochemistry of iron redox couple

Iron electrodes/electrolytes enable safety and environmental advantages when compared to other battery electrode/electrolyte materials such as nickel, cadmium, lead, and zinc, which are very harmful. As mentioned, the cell potential of the redox flow battery is highly dependent on the combination of the positive and negative redox couples. The schematic representation of the redox potential of various Zn-Fe conditions is shown in Figure 2.

View Article Online
DOI: 10.1039/D4YA00358F

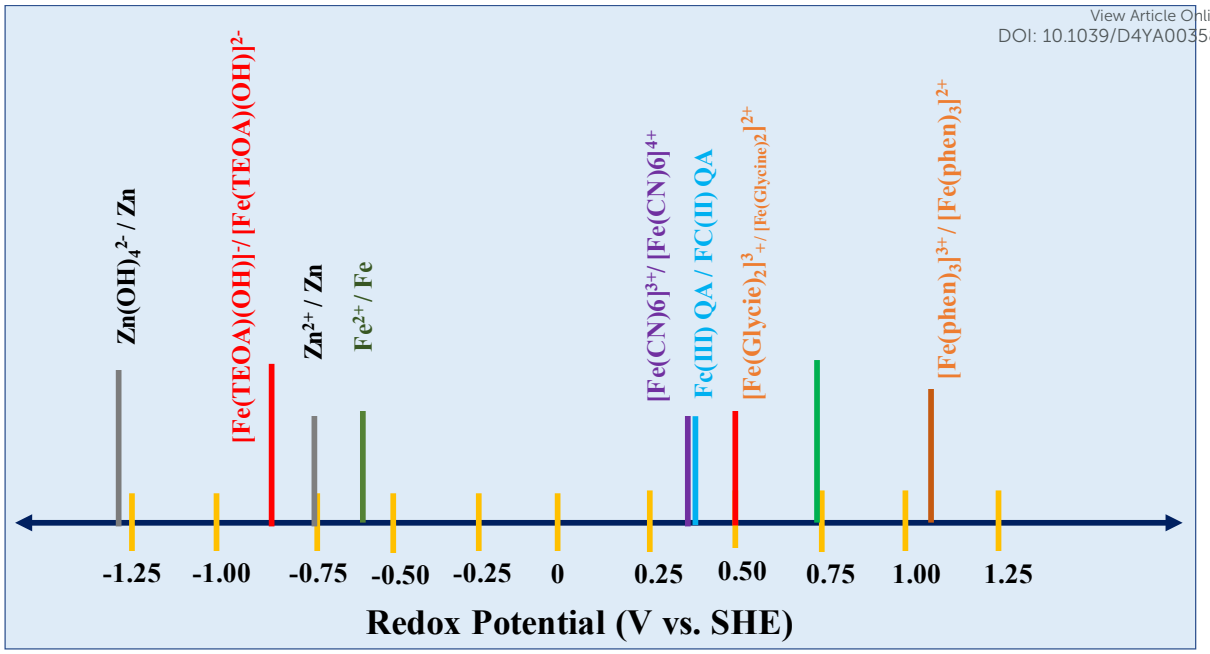

Figure 2. Schematic representation of redox potential of Zn and Fe at different conditions.

(a) Alkaline medium

In a rechargeable iron electrode, iron (II) hydroxide is reduced to iron during charging, while the opposite reaction occurs during discharge as shown below.

$$Fe(OH)_2 + 2e^- \rightleftharpoons Fe + 2OH^- \quad E^\circ = -0.87 \text{ V vs Hg/HgO} \quad \ldots\ldots\ldots (4)$$

The discharge product, iron (II) hydroxide, is oxidized to iron (III) hydroxide. Upon further discharge, it exhibits the reaction shown below.

$$Fe(OH)_3 + e^- \rightleftharpoons Fe(OH)_2 + OH^- \quad E^\circ = -0.56 \text{ V vs Hg/HgO} \quad \ldots\ldots\ldots (5)$$

The reaction in equ. (5) takes place at a very low cell voltage and so cannot be used to store energy. The conversion of iron (II) hydroxide to iron involves a plating/stripping mechanism[34]. During discharge, iron is oxidized to produce ferrite anion as shown in eqn (6). The resultant ferrite anion is very slightly soluble in an alkaline medium and further hydrolyzes to form iron (II) hydroxide as shown in eqn (7).

$$Fe + 3OH^- \rightleftharpoons HFeO_2^- + H_2O + 2e^- \quad \ldots\ldots\ldots (6)$$

$$HFeO_2^- + H_2O \rightleftharpoons Fe(OH)_2 + OH^- \quad \ldots\ldots\ldots (7)$$

View Article Online
DOI: 10.1039/D4YA00358F

The iron (II) hydroxide is electrically insulating and gets passivated on the electrode surface at high current densities; thus, it is necessary to prevent the electrode from being completely discharged. As the $Fe(OH)_2$ is thermodynamically unstable to form iron oxide as mentioned in equ. (8).

$$3Fe(OH)_2 \rightarrow Fe_3O_4 + 2H_2O + H_2 \text{ ……. (8)}$$

(b) Acidic/neutral medium

In an acidic medium, the iron electrolyte undergoes a reversible plating/stripping process. For example, 0.5M $FeSO_4$ solution of pH = 5.5 exhibits large polarization for the plating/stripping process because of the high energy barrier of ferrous dehydration and nucleation. Iron anode suffers more from parasitic reactions such as hydrogen evolution reaction (HER) than alkaline medium because of the high concentration of H^+ ions. The onset potential of HER in 0.5M $FeSO_4$ is -0.32 V, which is 0.12 V higher than that of the plating process. Hence, it is clear that during the plating process of iron, HER proceeds at a significant rate and so it affects the plating/stripping process resulting in very low coulombic efficiency.

$$Fe^{2+} + 2e^- \rightleftharpoons Fe \quad E^\circ = -0.44 \text{ V vs SHE ……. (9)}$$

$$2H^+ + 2e^- \rightleftharpoons H_2 \quad E^\circ = -0.32 \text{ V vs SHE ……. (10)}$$

On the other hand, aqueous Fe^{3+}/Fe^{2+} is one of the safest, low-cost, and widely used redox couples for positive electrode reactions with high reversibility even upon comparison with unmodified carbon electrodes[35]. The electrochemical process of the Fe^{3+}/Fe^{2+} redox couple is shown below.

$$Fe^{3+} + e^- \rightleftharpoons Fe^{2+} \quad E^\circ = +0.77 \text{ V vs SHE ……. (11)}$$

Though Fe^{3+}/Fe^{2+} redox couple is useful in energy storage, it cannot withstand high pH conditions due to precipitation as ferric hydroxide caused by HER at anode. So, the pH of the electrolyte has to be carefully maintained throughout the battery operations. Further, Fe^{3+} ions have a greater tendency to crossover from positive to negative side compartment that causes

self-discharge. Thus, coordinating ferric ions with suitable ligands can mitigate this situation[36-38].

2.3 Working principle of zinc-iron redox flow battery

Zinc electrodeposition occurs via distinct mechanisms in alkaline and neutral/acidic environments. The schematic representation of the Zn-Fe redox flow battery is shown in Figure 3. The detailed electrochemical reaction for zinc anode in different electrolyte mediums is described below.

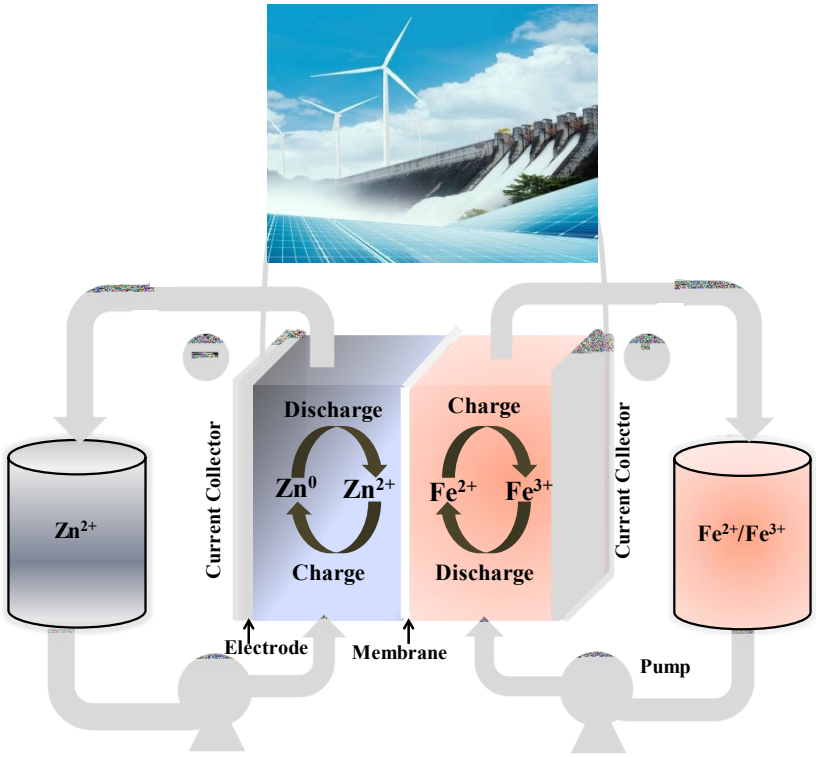

Figure 3: Working principle of the Zn-Fe Redox Flow Battery

It is critical to develop a novel flow battery technology with low-cost, high-energy density, and superior electrochemical activity. In this regard, zinc and iron are two widely available metals found in the earth's crust, which also exhibit excellent electrochemical characteristics. Thanks to the high solubility of the zinc and iron salts, it makes it easy to construct the battery to achieve high energy density. Further, zinc plating/stripping is relatively more stable than

View Article Online
DOI: 10.1039/D4YA00358F

iron plating/stripping, so using zinc as anode is highly beneficial over iron as it controls HER, fast kinetics with high coulombic efficiency, and low redox potential. The half-cell reactions for zinc-iron RFB occur at the anode and cathode which is represented below in eqn. (12) and (13)

At anode:

$$Zn^{2+} + 2e^- \rightleftharpoons Zn \quad E^\circ = -0.76 \text{ V vs SHE} \ldots\ldots\ldots (12)$$

At cathode:

$$2Fe^{2+} \rightleftharpoons 2Fe^{3+} + 2e^- \quad E^\circ = +0.77 \text{ V vs SHE} \ldots\ldots\ldots (13)$$

Net cell reaction:

$$Zn^{2+} + 2Fe^{2+} \rightleftharpoons Zn + 2Fe^{3+} \quad E_{cell} = +1.53\text{V} \ldots\ldots\ldots (14)$$

During the charging process, Fe^{2+} ions are oxidized to form Fe^{3+} ions at the positive electrode; whereas Zn^{2+} ions at the negative electrode receive these electrons from the external circuit and get electrodeposited as metallic Zn on the electrode. During the discharge process, reverse reactions occur at the corresponding electrodes. Since zinc anode involves a plating/stripping mechanism, it cannot decouple its energy and power density independently. Hence, it is considered a hybrid redox flow battery. Further, the zinc-iron flow battery has various benefits over the cutting-edge all vanadium redox flow battery (AVRFB), which are listed below: (i) the zinc-iron RFBs can achieve high cell voltage up to 1.8 V which enables to attain high energy density, (ii) since the redox couples such as Zn^{2+}/Zn and Fe^{3+}/Fe^{2+} show fast redox kinetics with high cell voltage, it is possible to test at high current density operations. So far, 260 mA cm^{-2} is the maximum operable current density[39], and (iii) alkaline zinc-iron RFB can attain a capital cost of less than \$90/kWh[40].

3 Challenges in Zn-Fe Redox Flow Batteries

There are various common issues such as low power density, low practical energy density, solubility and ion crossover between the compartments during cell operations have

View Article Online
DOI: 10.1039/D4YA00358F

been identified in any RFB systems. Zn-based RFBs also have a similar issue along with the Zn dendrite during the cell operation (Figure 4). These issues have to be addressed to obtain good-performing Zn-Fe RFBs.

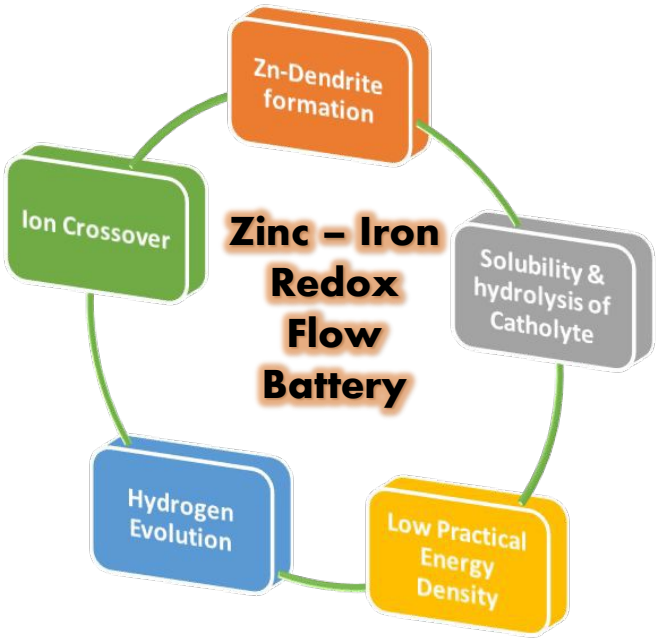

Figure 4: Various issues associated with the Zn-Fe redox flow batteries

(a) Zinc anode – Dendrite formation

The complications related to the zinc redox couple originate mostly from zinc dendrite and residual zinc deposits during cell operations which is one of the most vital concerns for zinc-based RFBs. The zinc dendrite/residual zinc deposits are more problematic in an alkaline medium than in a neutral or acidic medium, particularly at high current densities (> 60 mA cm^{-2}). During the charging process, zinc ions get electroplated on the electrode, and not all the plated zinc gets stripped off, but some zinc deposits remain intact in the electrode itself known as residual zinc, which affects the capacity of a battery and triggers inhomogeneous zinc plating followed by dendrite formation (Figure 5). Another major impediment in zinc anode is the restricted areal capacity and limited operating current density which have been evaluated in several viewpoints in recent years[41-42].

View Article Online
DOI: 10.1039/D4YA00358F

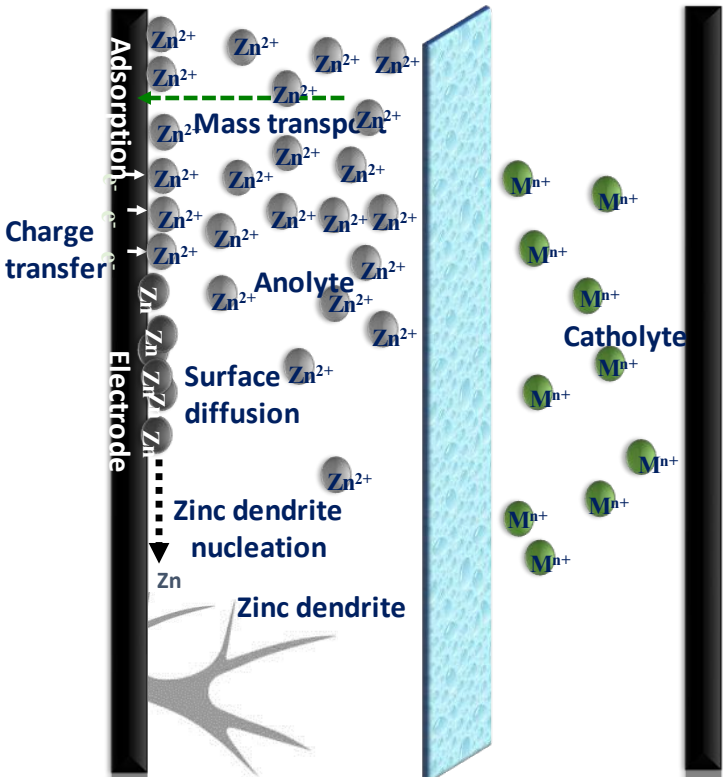

Figure 5: Schematic representation of the Zn-dendrite formation at the anode

(b) Membrane -Ion transfer

The ideal membrane for RFBs should have strong ionic conductivity, selectivity for ions, and great stability to provide a long lifespan. One of the most critical characteristics of membranes used in zinc-iron RFBs is their stability in alkaline medium, as most often highly concentrated alkaline condition (3M KOH or NaOH) is used for zinc-iron RFBs. As a result, the hydrocarbon polymer backbone and anion-exchange group can be deteriorated. Furthermore, Nafion series membranes have various disadvantages compared to the aforementioned alternative hydrocarbon-based membranes such as high cost and low conductivity in alkaline-based flow batteries[42-43]. Further, the selection of IEM or Separator is very important to avoid the various issues related to the Zn-Fe cell operations (Figure 6).

View Article Online
DOI: 10.1039/D4YA00358F

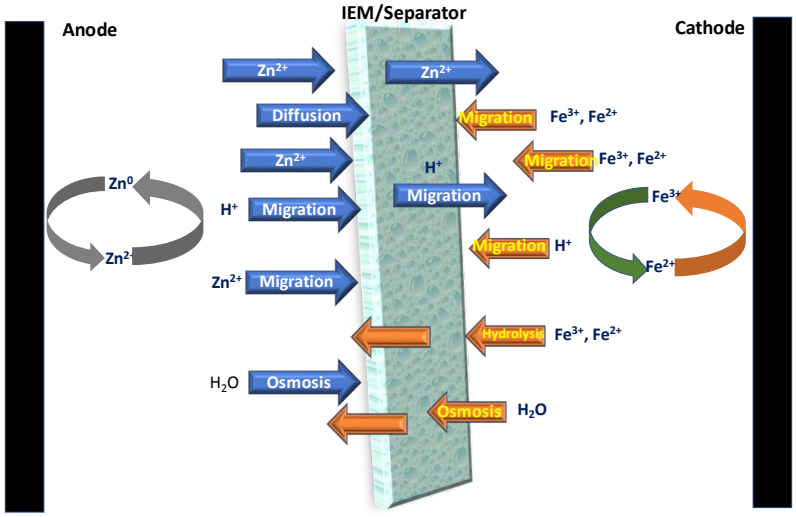

Figure 6: Schematic representation of various ions and molecules transfer through the separators during the cell operation of the Zn-Fe system

(c) Iron low solubility and hydrolysis at the cathode

The poor solubility of the ferro-ferricyanide redox couple in a [44]positive electrode result in low energy density. Changing the counter ions (K^+ or Na^+) of ferro-ferricyanide ions to ammonium ions is an effective technique for increasing the concentration of ferro-ferricyanide pair in aqueous solution. However, the instability of ammonium ions in a highly alkaline media makes it problematic to use in alkaline-based RFBs. The ferro-ferricyanide redox couple concentration in an alkaline medium is 0.4M, significantly lower than the concentration of vanadium ions 1.5 M in a vanadium flow battery[39-40]. On the other hand, ferric ions (Fe^{3+}) in the positive electrolyte (i.e., catholyte) are highly unstable at pH (> 4.5) as it leads to the formation of ferric hydroxide ($Fe(OH)_3$) as shown below in eqn. (15)-(17) and gets precipitated[26].

$$Fe^{3+} + H_2O \rightarrow Fe(OH)^{2+} + H^+ \ldots\ldots\ldots (15)$$

$$Fe(OH)^{2+} + H_2O \leftrightarrow Fe(OH)_2^{+} + H^+ \ldots\ldots\ldots (16)$$

$$Fe(OH)_2^{+} + H_2O \leftrightarrow Fe(OH)_3 + H^+ \ldots\ldots\ldots (17)$$

View Article Online
DOI: 10.1039/D4YA00358F

Further, Fe^{3+} ions have a greater tendency to crossover from the positive side to the negative side and initiate self-discharge of the battery[45]. Therefore, urgent steps have to be taken to mitigate the aforementioned issues.

(d) Water transfer through membrane/separator

The irreversible water transfer is another issue widely seen in RFBs. The differences in concentration gradient and ionic strength will arise between the positive and negative electrolytes, causing the battery to suffer from water transfer. This problem might reduce the battery performance significantly causing scarcity/imbalance of electrolytes. Thus, adding compounds to negative electrolytes or optimizing electrolyte ingredients to balance the disproportions in concentration gradient and ionic strength in electrolytes may be overcome by viable approaches to doggedness the problem of water transport[46-47].

(e) Hydrogen evolution Reaction (HER):

Hydrogen generation is one of the major concerns in RFBs. The parasitic HER reduces the capacity of the RFBs. Primary electrodes in the negative compartment (graphite or carbon felt) are subjected to thermal treatments to suppress the HER. Further, the H_2 gas molecules formation at the anode compartment restricts the electrolyte flow which increases the pressure inside the cell will be increased. Thus, it will encourage the overall cell resistance and leakage of the electrolyte, and hence, the cell performance will be strictly affected. Much attention is needed on the negative electrode electrolyte compartment to overcome this HER issue.

4 Progress of zinc-iron redox flow batteries

As previously stated, techniques for exploring advanced materials i.e., electrodes, electrolytes, and separators are critical in mitigating the concerns and challenges connected with zinc-iron RFBs, as the essential materials of RFBs ultimately decide the battery performance. The key requirements for any RFBs are given in Figure 7.

View Article Online
DOI: 10.1039/D4YA00358F

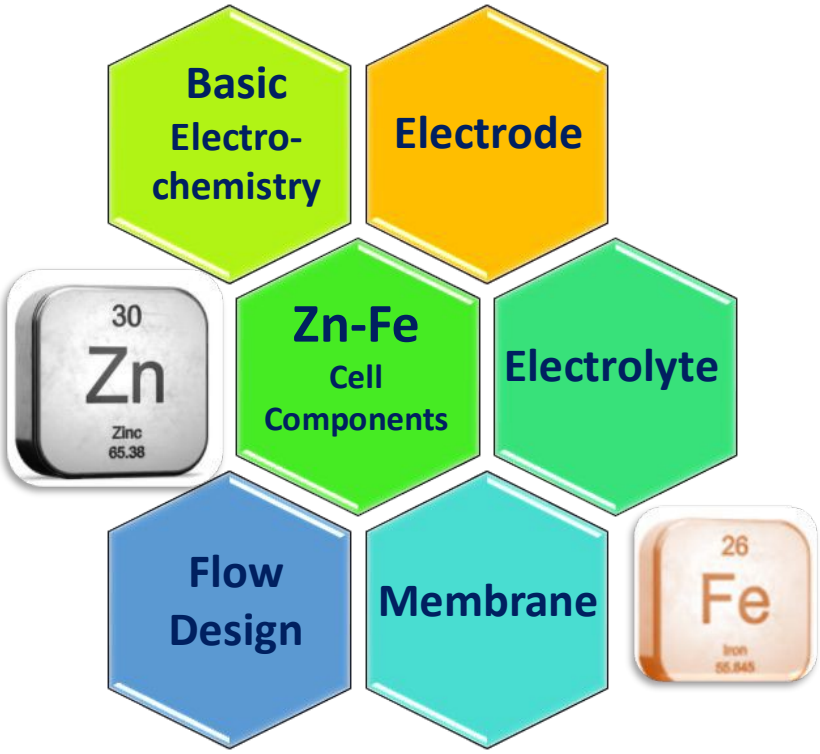

Figure 7: Key requirements for the RFB applications

4.3 Electrodes

The electrode is a key component in RFBs; it enables active areas for the redox processes to occur, but it does not take part in the reaction. The physicochemical characteristics of the electrode greatly influence the battery's performance[48-49].

Effects of zinc plates and carbon felt (CF) as electrodes in alkaline zinc-iron RFB were investigated[40]. The zinc plate brightly shows the phenomenon of unequal zinc deposition and the formation of zinc dendrites due to poor electrical conduction between the zinc plate and deposited metallic zinc. As a result, the deposited metallic zinc gets peeled off during the discharge process, resulting in zinc electrode deformation and corrosion. On the other hand, zinc deposit on the CF electrode shows uniform deposition of zinc due to high adsorption ability and a large specific surface area of CF. It also significantly reduces the internal interface resistance between the electrode and the deposited metallic Zn and promotes the diffusion of

View Article Online
DOI: 10.1039/D4YA00358F

OH^- ion due to the porous nature of CF. The zinc-iron RFB with CF shows an EE of 84.05 %, which is much greater than that of the Zn plate (78.52 %). A transient 2D mathematical model has been explored on the porous electrode in alkaline zinc-iron RFB. The alkaline zinc-iron RFB having a 7 mm thick anode and a 10 mm thick cathode with a porosity of 98 % exhibited energy, coulombic energy, and utilization rates of 92.84, 99.18, and 98.62 %, respectively[50]. Thus, the thick and highly porous electrode electrodes greatly enhanced the battery performance. Similarly, Beck et al.[51] used a 3D model of a porous electrode to create architecture electrodes that reduced power loss more than bulk electrodes due to porosity distribution optimization. The power efficiency of framework scaling from 4 cm^2 to 64 cm^2 was lowered by 12.3 % using the variable porosity electrode, but by 40.3 % when utilizing the uniform porosity electrode.

4.4 Membranes

Various types of membranes have been employed in energy storage applications. The membrane or separator can be classified based on the working mechanism or nature of the physical and chemical characteristics. The separators can be woven, non-woven, molded sheets and ribbed-type porous membranes, etc. Based on the pore size, the separator or membrane is classified as 1) microporous (50-100 Å). 2) non-woven (1-100 μm) and 3) ion-exchange membrane (> 20 Å)[52]. The selection of membranes or separators highly depends on the redox chemistry and the pH of the electrolyte combinations used in the battery.

The ion-exchange membrane (IEM) or separator in RFBs is a very essential for separating positive and negative electrolytes which also helps for charge-balancing by exchanging ions between the electrolytes in some special cases where IEMs are employed[53]. The ideal membrane or separator should have high ionic conductivity to reduce battery resistance, high ion selectivity to avoid self-discharge, chemical tolerance to withstand the highly alkaline environment, and high mechanical stability to protect the membrane from zinc dendrite

View Article Online
DOI: 10.1039/D4YA00358F

damage. In zinc-iron RFBs, Zn^{2+} (anolyte) and Fe^{2+}/Fe^{3+} (Fe^{n+}) (catholyte) ions are active redox couples shuttling between the membranes causing a capacity fade. It has to be noted that the radius of Fe^{n+} is 63-92 pm, which is much less than that of Zn^{2+} (139 pm). The Fe^{n+} ion permeability through Nafion was found to be 5.5×10^{-5} cm^2/min, which was 18.9~20.7 times greater than that of the vanadium ion (2.9×10^{-6} cm^2/min)[26]. Hence, Fe^{n+} crossovers are far easier than Zn^{2+} resulting in self-discharge of battery. The selection of membrane materials with special designs in the cell architecture can stretch the battery to a good performance.

a) Fluorinated ion-exchange membrane

A triple-electrolyte-designed flow cell was assembled with the combination of cation (Nafion 112 or Nafion 211) and an anion (FAA-3 or A901) exchange membranes. The neutral electrolyte is used as the middle electrolyte to control the pH of the anolyte and catholyte. Here the middle electrolyte helps to control the concentration polarization. During the charge, the CEM allows Na^+ to the negative half-cell and AEM allows the Cl^- to the positive half-cell from the middle electrolyte. This unique cell configuration significantly improves the concentration polarization resistance (R_{cp}) and Ohmic resistance (R_o). The concentration polarization of the middle electrolyte is gained again during the discharge process[54].

b) Porous and other common separators

Perfluorinated ion-exchange membranes are widely used in strongly acidic or alkaline conditions due to high chemical stability, however, it further increases the cost of the battery[55-57]. Polybenzimidazole (PBI) has recently emerged as a viable family of membrane materials for RFBs, because of its well-known outstanding chemical stability and mechanical robustness. The heterocyclic rings of a PBI membrane facilitate the fast ion transportation of hydroxyl ions. It was recently revealed that acid-doped PBI membranes used in all vanadium redox flow batteries (VRFBs) had remarkably minimal vanadium penetration and maintained outstanding long-term stability during cycling tests for 13,500 cycles[58-60]. In this connection, Yuan et al.[40],

View Article Online
DOI: 10.1039/D4YA00358F

demonstrated a low-cost PBI membrane in alkaline zinc-iron RFB with CE of 99.5 % and EE of 82.8 % at 160 mA cm^{-2} that can withstand over 500 cycles. The feasibility of this battery is demonstrated by manufacturing a kilowatt cell stack with a capital cost of less than $90/kWh. Moreover, the use of porous ion-conducting membranes instead of conventional IEMs reduces the problem of internal resistance of the membrane due to facile ion transport, which greatly improves the performance and stability of Zn-Fe RFBs. Remarkably, the cost-effective porous separator utilization can decrease the cost of zinc-iron RFBs to less than $50/kWh. Recently, a microporous separator (Daramic 175, thickness 175 μm) was employed to separate the anode and cathode compartment of the flow cell[61]. Yuan et al.[62] created a nanoporous separator with negative charges in the pore surface and wall. The separator induces the deposition of zincate ions to the CF framework by mutual repulsion between the separator's pore surface/walls and the zincate ions $Zn(OH)_4^{2-}$. As a result, even if zinc dendrites emerge, they grow through the rear end of the separator, avoiding separator breakage and the zinc-iron RFB short-circuit phenomena. Using a negatively charged nanoporous membrane results in no zinc dendrites at 80-160 mA cm^{-2} after 240 cycles. To increase the conductivity of the membrane, a cation on the pristine SPEEK membrane wherein H^+ is changed to K^+ and used in zinc-iron RFB application. Though the main focus is on the SPEEK membrane, the flow cell is also tested using Nafion 117 and compared with the SPEEK-K-based Zn-Fe flow cell performance. The discharge capacity of the cell for the SPEEK-K membrane-based cell is much better (16.4% higher) than the Nafion 117-based cell configuration. However, the cell was tested up to only about 30 cycles[63]. Minghui Yang et al.[64] elaborate the performance using KBr as a supporting electrolyte where the nafion 212 membrane is modified by exchanging the cation form H^+ to K^+ by soaking in 1 M KOH for about 1 hr at 80 °C. The K^+ exchange nafion 212 membrane was employed and the cell was tested up to 2000 cycles which showed stable performance with a CE of nearly 100 % at capacitance retention of >80 %. A similar ion exchange process was

View Article Online
DOI: 10.1039/D4TA00358F

followed where Na^+ is attached and the treatment was carried out in NaOH solution and used in the Zn-Fe flow cell investigation[65]. On the other hand, Nafion 212 was used in the flow cell and the cell was tested up to 100 cycles[66]. The use of condensing guanidine carbonate with formaldehyde followed by cross-condensation with melamine AEM allowing only the Cl- exchange from anolyte to the catholyte showed no dendrites during the charging process. On the other hand, the porous PVC membrane-based cell showed a dendrite formation even from the first cycle[67]. It was observed that the ion-selective ability of the AEM membrane highly influences the uniform deposition of the zinc during the charge on the anode[62, 68-69]. The positive and negative half-cells were separated by a perfluorinated sulfonic acid membrane (Liaoning Keking New Materials, China) to prevent the ion crossover[70]. Chen et al[71] used the crosslinked and methylated polybenzimidazole (PBI) anion exchange membrane (~40 μm thick) and the developed flow cell showed 100% CE and was tested up to 150 cycles. However, the cell was tested at a maximum current density of 20 mA cm^{-2} only.

A non-ionic ion-exchange membrane (n-IEM) has been employed to separate the anode and cathode compartment in which the alkaline electrolyte has been employed. The poly (ether sulfone) (PES) based membrane with high ion conductivity and anti-alkali stability was prepared and used for alkaline Zn-Fe RFB where polyethylene glycol (PEG) was used as an additive. The non-ionic membrane based flow cell was tested at 80 mA cm^{-2} about 120 cycles in an alkaline memdium[72]. These findings confirm that the n-IEM has the potential for alkaline RFBs. Similarly, the microporous celgard membrane and Nafion 115 cation exchange membranes were investigated in the zinc-iron flow cell. The obtained result showed much better performance while using the Nafion 115 while the cell showed very poor performance when employing the microporous separator. The flow cell showed a CE of > 90 % and VE of > 86 % over 20 cycles, and the cell showed capacity retention of 80 % after 200 cycles when using the Nafion 115 membrane[73].

View Article Online
DOI: 10.1039/D4YA00358F

4.5 . Electrolyte

As mentioned earlier, in conventional batteries, energy is stored in the electrodes whereas in RFBs the rated energy is determined by the electrolytes. The solubility of the redox active species and the redox potential of the electrolytes determine the capacity and efficiency of the system. Further, the pH of the electrolyte also plays a vital role in determining the cell voltage, as it alters the electrode potential. For instance, the Zn/Zn^{2+} redox reaction in a neutral electrolyte medium occurred at -0.76 V vs SHE, whereas it happened at -1.245 V vs SHE in an alkaline medium. On the other hand, the positive redox couple of Fe^{3+}/Fe^{2+} occurs at +0.744 V vs. SHE. Therefore, on combination of the Zn/Zn^{2+} with Fe^{3+}/Fe^{2+} as anolyte and catholyte, establishes a cell voltage of 1.52 V and 2 V at neutral and alkaline electrolyte medium of Zn^{2+}/Zn, respectively. In a zinc-iron RFB system, the electrolytes at different pH have been employed, specifically, the alkaline-based anolyte has attracted much attention due to the high reduction potential of Zn/Zn^{2+}. On the other hand, neutral electrolytes preferred the additives on the catholyte side. A sharp increase in the charge potential was observed resulting in the irreversible HER in the negative half-cell. The HER results from the corrosion of zinc in alkaline solutions. The corrosion of zinc is the main cause of the self-discharge of secondary alkaline zinc-based batteries. To suppress the HER at the anode, many organic and inorganic additives have been employed; on the other hand, the addition of the additives also helps to balance the water transport between the half-cells. Systems of organic additives have been largely investigated at different conditions which shows a highly improved performance. The

View Article Online
DOI: 10.1039/D4YA00358F

CV curve recorded at 20 mV s^{-1}, the peak current density, potential, and current density are shown in Figure 8.

Figure 8. Electrochemical performance comparison of Fe(II) complexing ligands by CV measurements for 20 cycles at a scan rate of 30 mVs^{-1}: (a) CV curves (the average), (b) anodic and cathodic peak potentials (Epa, Epc) (c) anodic and cathodic peak currents (Ipa, Ipc), and (d) peak current ratio. [Reproduced with Permission[66]]

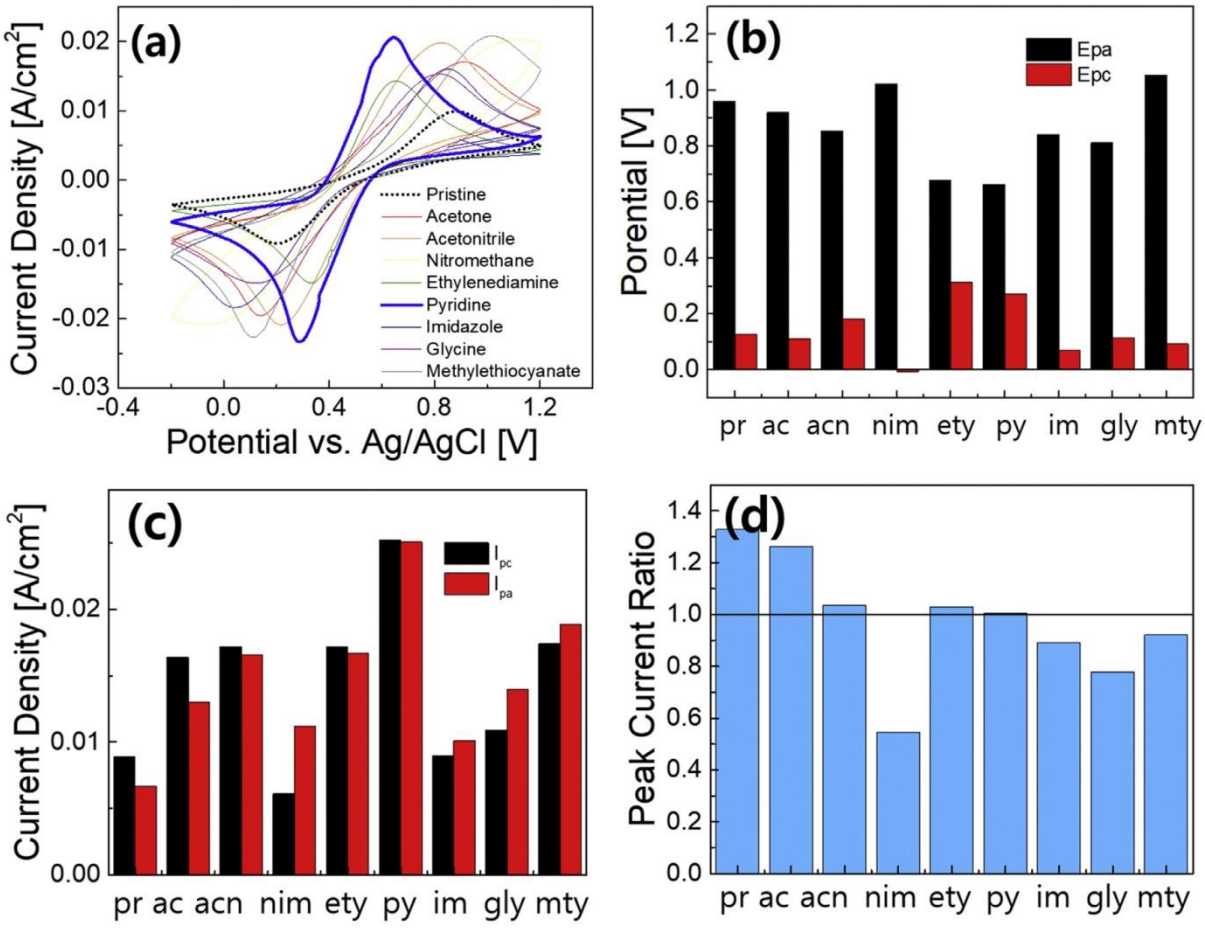

† pristine (pr), acetone (ac), acetonitrile (acn), nitromethane (nim), ethylenediamine (ety), pyridine (py), imidazole (im), glycine (gly), methyl-thiocyanate (mty)

The Zn-Fe RFB showed 1.8 V cell voltage when designed using the triple-electrolyte combinations. The redox behavior of iron species has been tested in aqueous ionic liquid solutions. 1-butyl-3-methylimidazolium chloride (BMImCl) is found to be most effective in regulating the redox activity of iron species. While in the anolyte, the standard rate constant of zinc plating/stripping was promoted to 1.44×10^{-4} cm s^{-1} when aqueous 1 M NH_4Cl is used as

a supporting electrolyte; The flow cell exhibits a highly stable cycle over 150 cycles with a energy efficiency of 80 % at 20 mA cm^{-2} in a BMImCl/H_2O in HCl and $CaCl_2/H_2O$ in NH_4Cl (0.5 M), anolyte and catholyte respectively[71]. Alkaline Zn-Fe RFB was developed in which 1.0 $molL^{-1}$ $Na_4Fe(CN)_6$ in 3 $molL^{-1}$ KOH and 0.5 $molL^{-1}$ $Zn(OH)_4^{2-}$ in 4 $molL^{-1}$ NaOH have been employed as catholyte and anolyte electrolytes, respectively. The high alkaline nature was superintendent the effective zinc stripping/plating which effectively suppressed zinc dendrite formation at the anode. Thus, this battery demonstrates a coulombic efficiency of 99.5 % and an energy efficiency of 82.8 %, and the cell was tested at 160 mA cm^{-2}. The RFB was tested up to 500 cycles with a cell voltage of 1.74 V[40].

With beneficial fast redox kinetics of the $Zn(OH)_4^{2-}/Zn$ and $Fe(CN)_6^{3-}/Fe(CN)_6^{4-}$ couples in an alkaline medium, the battery displayed no signs of activation polarization. Here, KBr is used as a supporting electrolyte on both sides. The combination of the electrolytes showed cell performance over 2000 cycles without any noticeable capacity loss at 30 mA cm^{-2}. Further, a stack having three cells was fabricated and the cell life was recorded up to 600 cycles[64]. The cells with 0.8 mol L^{-1} $Na_4Fe(CN)_6$ 3 M mol L^{-1} KOH solution and 0.8 mol L^{-1} $Na_2Zn(OH)_4$ in 4 mol L^{-1} NaOH solution were used in positive and negative electrolytes, respectively. The cell was tested at a maximum current density of 180 mA cm^{-2}. The cycle performance was analyzed at 80 mA cm^{-2}. The RFB demonstrated up to 150 cycles delivering a CE of 98.53%, a mean EE of 83.15%. The cell also showed stable performance up to 100 cycles even at 160 mA cm^{-2} [72]. $K_4Fe(CN)_6$ is identified as a highly suitable active electrolyte component in the positive electrolyte. However, the solubility of $K_4Fe(CN)_6$ in alkaline electrolyte is limited due to the common ion effect. The solubility of $K_4Fe(CN)_6$ was increased by employing a diverse ion effect. Therefore, to increase the solubility, NaOH was employed as a solvent. Higher solubility of 1.6 M $K_4Fe(CN)_6$ in 0.5 M NaOH was obtained promoting high reversibility of $Fe(CN)_6^{4-}/Fe(CN)_6^{3-}$. A highly concentrated catholyte solution [1.46 M

View Article Online
DOI: 10.1039/D4TA00358F

$Fe(CN)_6^{4-}$ from a mixture of 1.15 M $K_4Fe(CN)_6$ and 1.15 M $Na_4Fe(CN)_6$ in 0.5 M NaOH was employed as the catholyte. The flow cell then showed a maximum capacity retention of 98.51% with CE, VE, and EE of 100%,83.43%, and 83.37% even after 124 cycles tested at 100 mA/cm^2. A maximum power density of 656.81 m W/cm^2 was obtained at 1.0 M $K_3Fe(CN)_6$ in 1.0 M NaOH. Jeena et al.,[67] investigated the Zn-Fe using 1 M Zn(II) chloride and the mixture of 0.5 M $FeCl_2$ and 0.5 M $FeCl_3$ with 2 M NH_4Cl as anolyte and catholyte. Here, NH_4Cl was added to the positive electrolyte as a supporting electrolyte to improve the conductivity of the electrolyte. The cell delivered a maximum energy efficiency of 81% 15 mA cm^{-2}. However, the cycle life was tested only up to 32 cycles. The high reversibility of Zn was realized on carbon felt electrodes for zinc−iron RFBs by introducing nicotinamide (NAM) as an additive to neutral $ZnCl_2$ anolyte. The addition of NAM not only enhances the Zn striping/plating reaction but also helps to improve power density (185 m W cm^{-2}), good cycle life stability (400 cycles) with an energy efficiency of the flow cell around 70% at 50 mA cm^{-2}. The figure below (Figure 9) shows the cell performance at different conditions investigated by Tang et al.,[70].

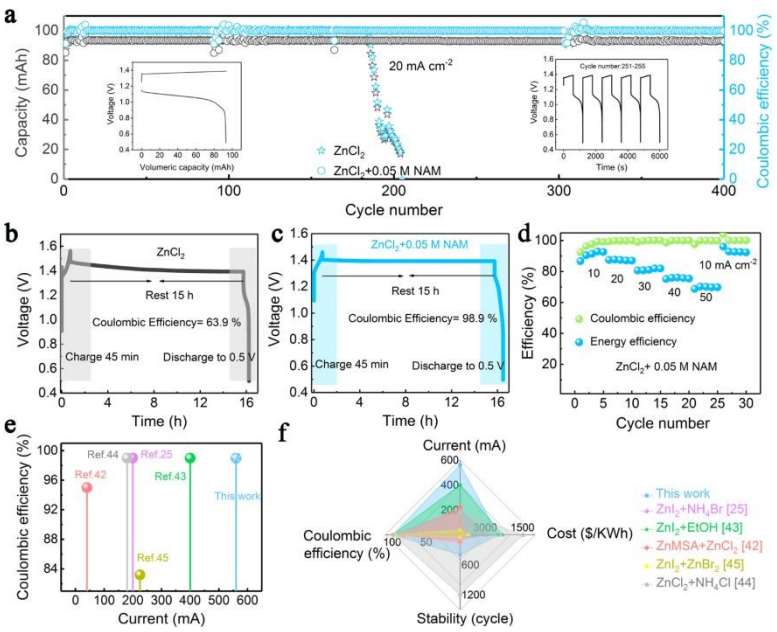

Figure 9: (a) Long-term cycling tests of the Zn-Fe RFB at 20 mA cm^{-2}. (b and c) Long standby tests of the Zn-Fe RFB using pure $ZnCl_2$ and $ZnCl_2$-NAM. (d) Rate performance of the Zn-Fe

RFB adopting a mixed $ZnCl_2$ and NAM anolyte at 10−50 mA cm^{-2}. (e and f) Comparison of the proposed Fe-Zn flow cell with other reported Zn-based RFBs.[Reproduced with permission from[70]]

To obtain a long cycle life and improved performance of the flow cell, pyridine was used as a Fe(II) complexing agent in the positive electrolyte. Pyridine ligand was coordinated with Fe^{2+} helped to improve the reversibility of the F^{2+}/F^{3+} redox reaction. The pyridine pyridine-incorporated electrolyte system delivered excellent performance when compared with the pristine electrolyte. The cell delivered an energy efficiency of around 80% up to 100 cycle[66]. On the other hand, 0.1 mol L^{-1} $Zn(OH)_4^{2-}$ + 1 mol L^{-1} OH^- and 40 mL of 0.4 mol L^{-1} $Fe(CN)_6^{4-}$ + 1 mol L^{-1} OH^- have been employed as anolyte and catholyte, respectively. Long-term cycle stability of the flow cell was recorded at 140 mA cm^{-2} up to 500 cycles. The flow cell delivered nearly 100% CE and about 80% of EE[74]. The $ZnCl_2/Fe(bpy)_3Cl_2$ based RFB delivered a CE > 90% and a voltage efficiency of >86% over 20 cycles and around 80% capacity retention was observed even after 200 cycles[73]. The key performances of the Zn-Fe RFBs are compared in Table 1. Zhang et al.,[64], investigated the Zn-Fe RFB using the $FeCl_2$ in BMImCl with 1 M HCl as a catholyte and $ZnCl_2$ in 3.5 M $CaCl_2$ with 0.5 M NH_4Cl as anolyte. It was observed that the addition of BMImCl/H_2O with the anolyte solution highly increased the reaction kinetics of the Zn plating and striping[71]. It is believed that the addition of the complexing additives further will improve cell performance where the additive should be inactive electrochemically to avoid any side reactions. The additive should be complexed with the main electrolyte component and chemically reversible during the cell operation.

View Article Online
DOI: 10.1039/D4YA00358F

6.4 Zn-Fe Stack performance:

Zn-Fe RFBs have been demonstrated at the stack level due to their excellent optimized cell performance representing them as a major competitor in the commercial market soon. To ensure this low-cost, eco-friendly, Zn-Fe RFB system, stack cells at various conditions have been analyzed at different cell levels. A three-cell stack was fabricated and their electrochemical performance was recorded. Photograph of the flow cell stack and its cycle life performance is shown in Figures 10a and 10b. With a stack voltage of 3.9 V, the cell stack showed a stable performance over 625 cycles with a CE of 99.0% at 30 mA cm^{-2} [64].

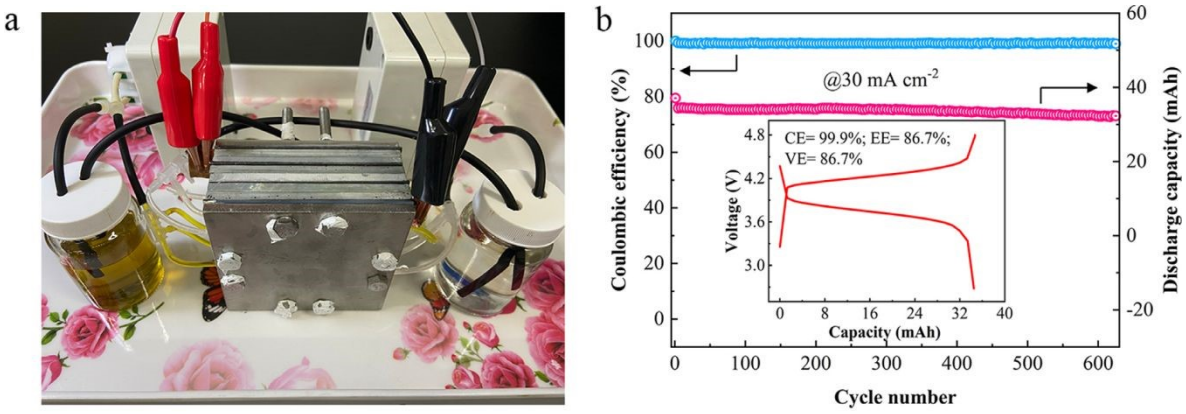

Figure 10. (a) A photograph of neutral Zn/Fe RFB stack. (b) Cycling performance of the cell stack with an insert of the 10th charging/discharging curves [Reference[64]]. [Reproduced with permission[64]].

The practical viability of the alkaline Zn-Fe RFB was ensured by making ten cells stacked with the help of the self-made PBI membrane. The stacked cell was charged at 20 V and showed an average discharge voltage of 16.10 V when tested at a current density of 80 mA cm^{-2}. The flow showed CE, EE, and VE of 98.84%, 84.17%, and 85.16%, respectively at a current density of 80 mA cm^{-2}, with an output power of 1.127 kW[40]. Photographs of the flow cell stack and the cell performance are given in Figure 9a-c. GCD profile, continuous GCD cycle, and the efficiencies vs cycle life are shown in Figure 9b-c.

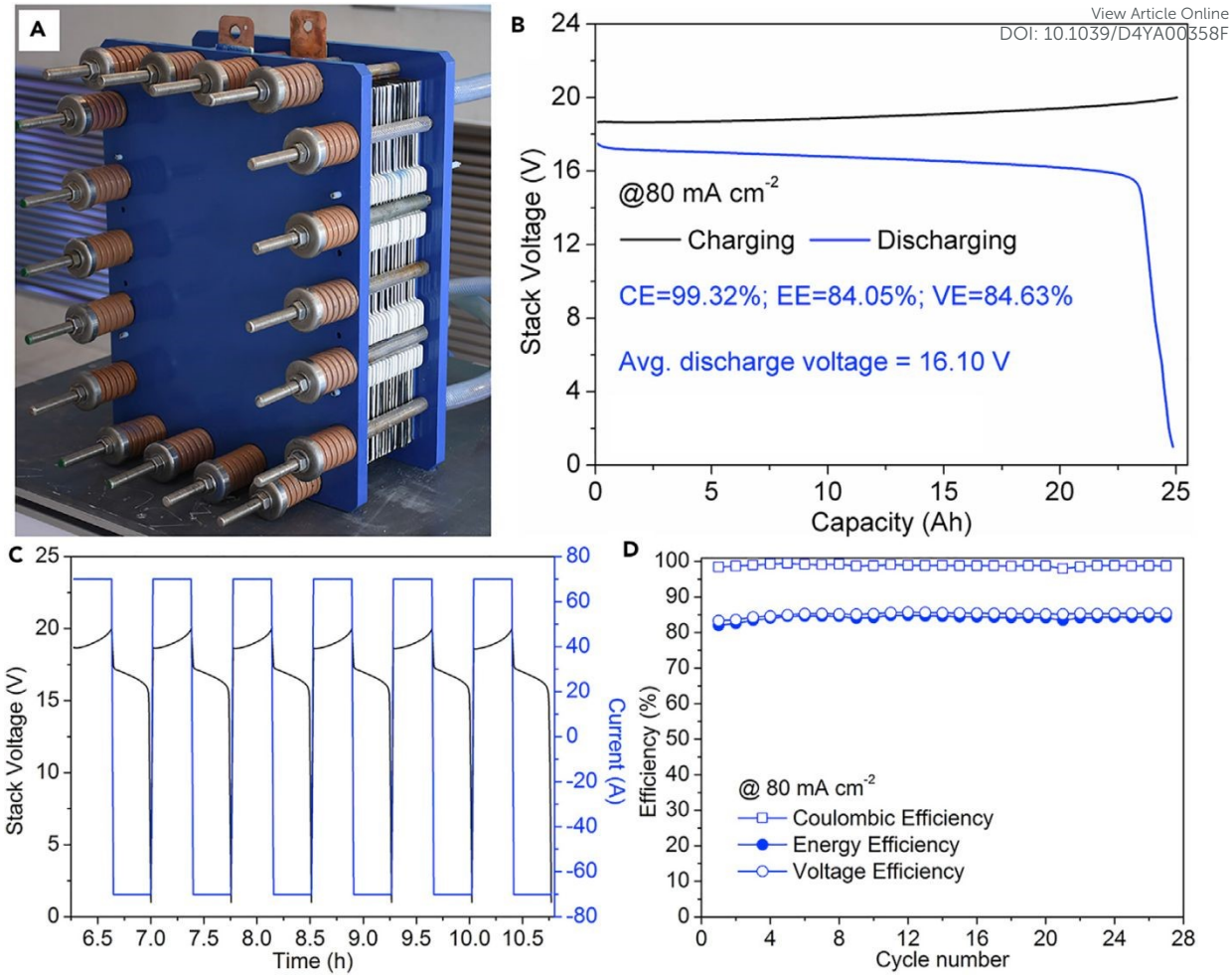

Figure 11. Practical Realization of the Alkaline Zinc-Iron Flow Battery: (A) The kW alkaline zinc-iron flow battery cell stack prototype using a self-made, low-cost non-fluorinated ion-exchange membrane. (B) Cell stack voltage profile of the alkaline zinc-iron flow battery at a current density of 80 mA cm-2. (C) Parts of charge and discharge curves of the cell stack. (D) Cycle performance of the cell stack at a current density of 80 mA cm^{-2}. [Reproduced with permission[40]].

A cell stack was fabricated and its electrochemical performance was analyzed using an alkaline electrolyte. In the stack cells, a high concentration of catholyte was employed where 1M NaOH was used as a solvent. The photograph of the flow cell stack and capacity vs voltage profile of the flow cell stack at the 10th and 100th cycle and the efficiency vs cycle number is shown in Figure 10 (a-c)[40].

View Article Online
DOI: 10.1039/D4YA00358F

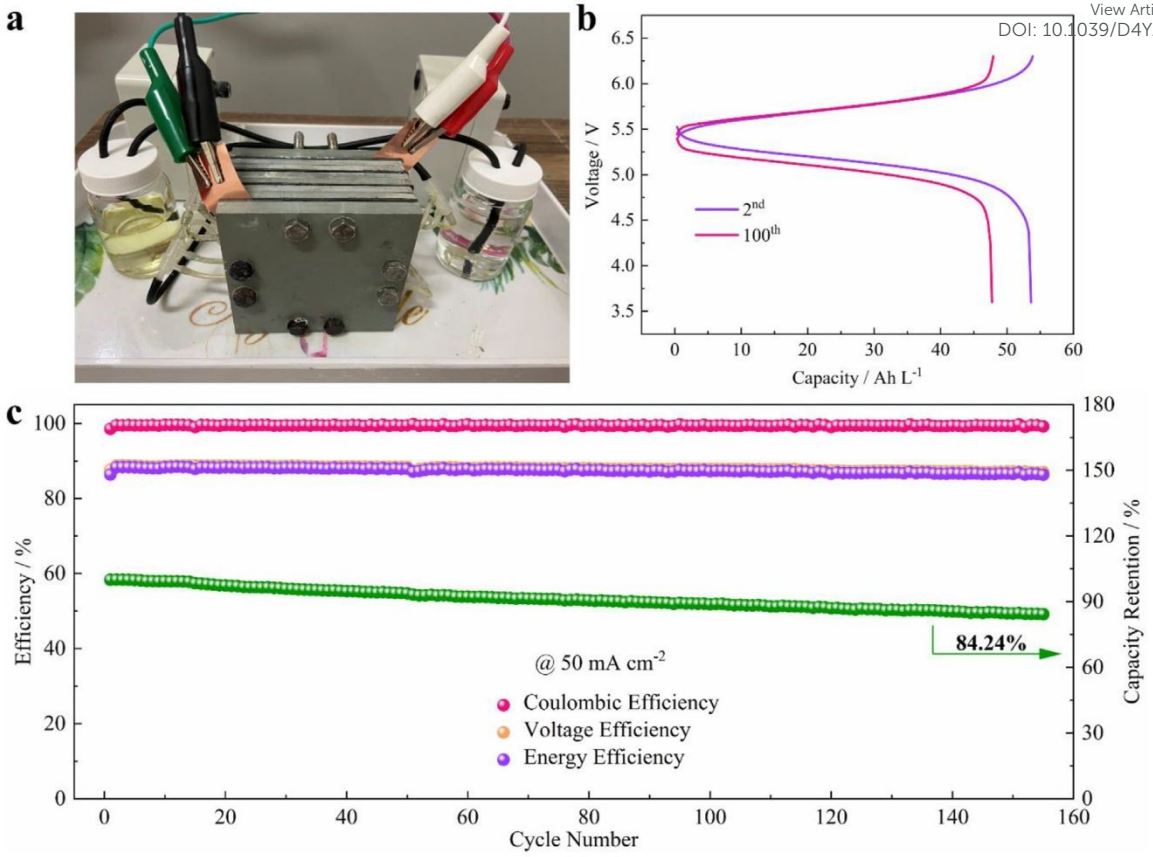

Figure 12. Practicability analysis of the AZIRFB system with high-concentration catholyte. (a) A photograph of the AZIRFB cell stack. (b) Selected charge-discharge voltage curves of the cell stack at 50 mA cm^{-2}. (c) Cycling performance of the cell stack at 50 mA cm^{-2}. [Reproduced with permission [65]].

6.5 Cost analysis comparison:

Further, Tan et al.[75] modeled the flow cell stack at various conditions. The modeled flow cell is also shown in Figure 13. Thus, the low-cost Zn-Fe RFB will become a suitable replacement for the expensive all-vanadium redox flow battery. However, various challenges have to be addressed before bringing it into the commercial perspective.

View Article Online
DOI: 10.1039/D4YA00358F

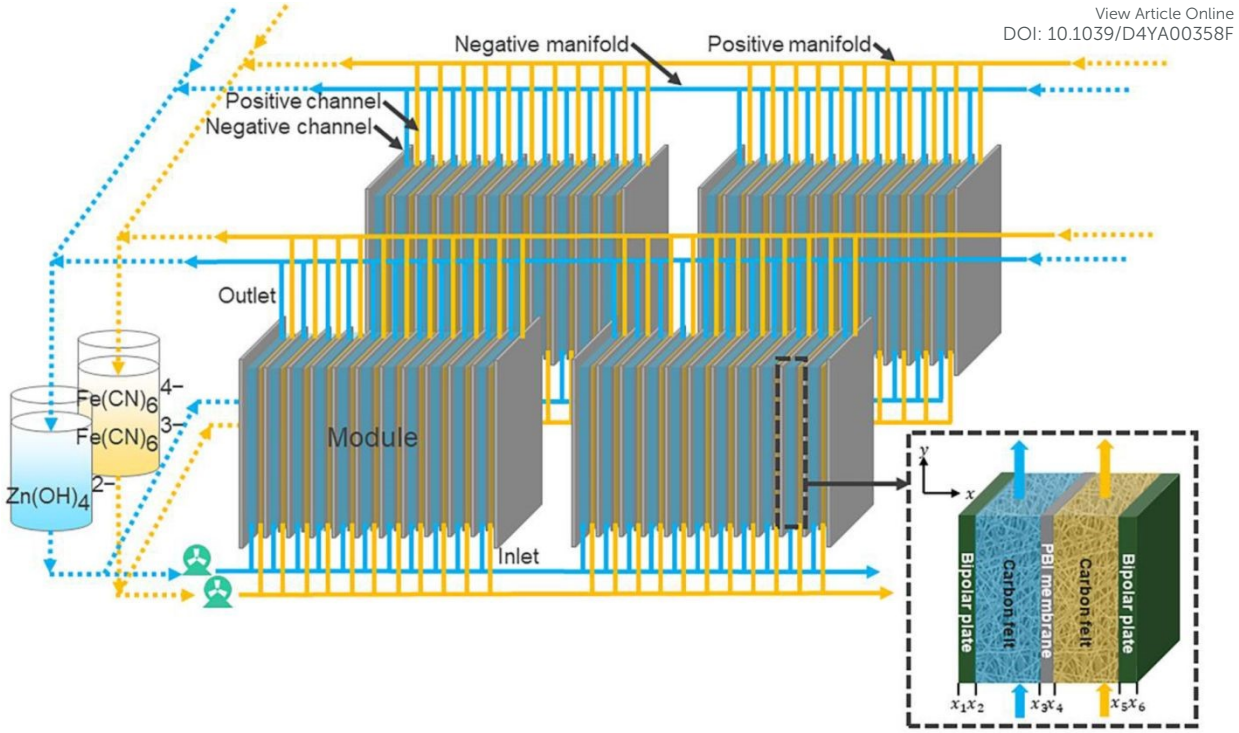

Figure 13. Schematic of a zinc-iron flow battery stack. [Reproduced with the permission[75]]

The capital cost of the Zn - Fe RFB was analyzed and compared with other redox flow batteries (Figure 14). It was observed that among the other large-scale energy storage systems, Zn-Fe showed highly efficient overall capital cost ($/kW-hr) at low current density[54].

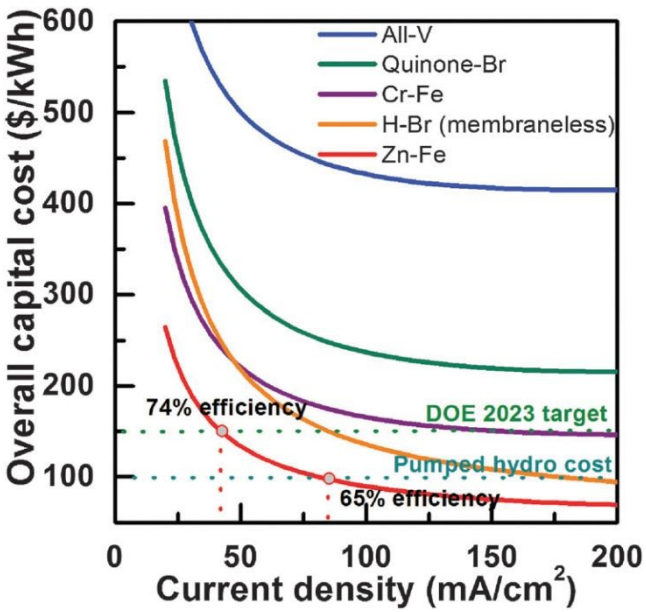

View Article Online
DOI: 10.1039/D4YA00358F

Figure 14. Zn–Fe RFB cost analysis and comparison with other notable RFBs. Note that long-term durability was not considered in the cost analysis in this work, and the cost comparison among different RFB technologies is only meaningful when they have the same or similar durability. (Reproduced with Permission[54]).

Future Perspective

A constant and continuous effort is needed to improve the Zn-Fe RFB cell performances. An effort should be made on all the key aspects including electrode, electrolyte, cell design, and operating conditions. Since the energy is determined by the redox nature of the couples, special attention should be given to the investigation of the redox couples such as Zn^{2+}/Zn and Fe^{3+}/Fe^{2+}.

i) Redox couple: To enhance the cell performance the redox couple environment has to be carefully evaluated. The pH of the electrolyte component plays a major role in the determination of the cell voltage of the redox flow battery. For instance, the Zn/Zn2+ redox reaction occurred at 0.76 V and 1.26 V in neutral and alkaline electrolyte medium. Due to the high electrode potential, an interest in the alkaline-based Zn has largely increased in the past few years. However, the Zn dendrite is still being a major concern. To suppress the Zn-dendrite, the electrode can be modified where a smooth Zn deposition is possible. The roughness of the electrode materials has to be controlled during the modification process. In most cases, the carbon felt has been heating at a very large temperature, which creates more defects on the surfaces. This will strictly affect the cell performance; therefore, the defect formations should be controlled by limiting the activation process. The elected conductivity is also very important to operate the cells at rated high current density. On the other hand, the electrolyte component can also be modified and additives can be incorporated to control the dendrite formation. To control and understand the formation of the Zn dendrite, advanced materials characterizations might be

used to characterize the interface interactions, particularly at the negative electrodes.

i. Iron hydrolysis: To develop a good performing catholyte, it has to be subjected to severe analyses in terms of the electrode reaction mechanism at different pH and additive environmental conditions. For example, in the case of Fe^{3+}/ Fe^{2+}, iron hydrolysis, is a major issue. A detailed working mechanism using theoretical calculations has to be carried out for an in-depth understanding of the side reactions. Additionally, in-situ characterization techniques are required to evaluate the iron-complexation process in depth. The selection of solvent specifically in an alkaline electrolyte medium is very important. As discussed, the precursor or source material of Fe is very important to execute the better performance of the flow cell.

ii. Supporting electrolytes has a huge research gap due to the influence on the determination of the flow cell performance. Different organic and inorganic additives have been investigated so far in various RFB applications. As mentioned, the additives should have good conductivity and electrochemically inactivity, at the same time, they should have good chemical reversibility to avoid a side reaction at the electrode.

iii. The development of low-cost membranes is the most crucial part of achieving scalability for Zn-Fe RFB. The study and development of membrane materials with strong mechanical properties, and self-recovery capabilities is of high priority. Innovative polymers, through molecular design, are still required to provide high-performance membranes for zinc-iron RFB applications. The porosity has to be controlled for the porous membranes, and the stability of the IEMs should be improved to have good performance in the high-risk condition of the RFB.

iv. Molecular modeling on electrolyte components, and separators (to obtain optimum porosity), is very important to obtain good-performing RFBs. Flow cell design will be

View Article Online
DOI: 10.1039/D4YA00358F

another important role where the width and depth of the flow fields play a very important role in the physical and mechanical aspects of the flow cell performance. The felt electrode thickness is another important factor where the pressure built in the cell compartment is carried by the 3D porous structure of the felt electrode. The key components may be optimized further using new artificial intelligence (AI) and machine learning tools. Along with the molecular modeling and DFT studies will further understand the effective electrolyte additive components.

v. Hydrogen evaluation is another important issue that has to be suppressed during the cell operation. To overcome this issue, the Graphite composite plate may be prepared by having a few wt% of the additives which can suppress the hydrogen evolution during the cell operation. The addition of additives or the catalyst with the HER-suppressed elements is likely Bi, Sn, Sb, Pb, etc. will improve the cell performance.

Thus, to meet the global energy demand Zn-Fe redox flow batteries will be one of the highly suitable sustainable energy storage systems. However, its future development will be dependent on solving zinc dendrites, iron (III) hydrolysis, and finding robust membranes that fulfill the primary economic and technological criteria of cost, power density, efficiency, and durability of the RFBs.

Table 1. Comparison of characteristics and the electrolytes of Zn-Fe RFBs.

S. No.	Electrolyte		Separator	Efficiency (%)	Cycle Life	Ref.
	Anolyte	Catholyte				
01.	0.6M $FeCl_2$ + 0.5 M NaCl + 1M HCl	0.3M $Na_2[Zn(OH)_4]$ + 0.5 M NaCl + 2.4M NaOH	Nafion-212 and FAA3	99.9 (CE), 76 (VE) at 80 mA cm^{-2}	20 Cell Stack	54
	Middle electrolyte: 3M NaCl					
02.	1M $ZnBr_2$ + 2M KCl	2M $FeCl_2$ + 4M Glycine + 2M KCl	polybenzimidazole porous membrane	97.75 (CE), 86.66 (EE) at 40 mA cm^{-2}	100	76
03.	0.1M $ZnBr_2$ + 2M KCl	0.2M $FeCl_2$ + 0.4M glycine + 2M KCl	SPEEK-K type membrane	95 (CE), 78 (EE) at 40 mA cm^{-2}	30	63
04.	0.1 M $ZnBr_2$ + 4.0 M KBr	0.1M $K_3Fe(CN)_6$ + 3M KBr	Nafion-212	99.9 (CE) at 30 mA cm^{-2}	320	64
05.	1.6M $ZnCl_2$ + 0.8 M $FeCl_2$ + 2M NH_4Cl + 2g PEG_{8000}	1.6M $ZnCl_2$ + 0.56M + $FeCl_2$ + 0.24M $FeCl_3$ + 2M NH_4Cl + 2g PEG_{8000}	microporous separator (Daramic 175)	85 (CE)	125	61
06.	0.5M $Zn(OH)_4^{2-}$ + 4M NaOH	1L $Na_4Fe(CN)_6$ + 3M KOH	Polybenzimidazole membrane	99.5 (CE), 82.8 (EE) at 160 and 80 mA cm^{-2}	500	40
07.	1M $ZnCl_2$	0.5M $FeCl_2$ + 0.5M $FeCl_3$ + 2M NH_4Cl	Anion exchange membrane	92 (CE), 85 (VE), □78 (EE) at 25 mA cm^{-2}	30	67

08.	0.5M $ZnCl_2$ + 0.05M nicotinamide (NAM) + 3M KCl	0.5M $K_4Fe(CN)_6$ + 1M KCl	perfluorinated sulfonic acid membrane	70 (EE) at 50 mA cm^{-2}	400@20 mAcm-2	70
09.	1.6M $ZnCl_2$	0.8M $FeCl_2$ + 0.8M Pyridine	Nafion-212 membrane	94.57 (CE), 81.26 (VE), 76.82 (EE)	100	66
10.	0.8M $Na_2Zn(OH)_4$ + 4M NaOH	0.8M $Na_4Fe(CN)_6$ + 3M KOH	Non-ionic poly(ether sulfone) (PES) membrane & polyethylene glycol (PEG) as additive	99 (CE), 87 (EE) at 80 mA cm^{-2}	150	72
11.	0.2 M $ZnBr_2$ in 4.0 M NaOH	0.1 M $K_4Fe(CN)_6$ in 1.0 M NaOH	Nafion-212 membrane	88.10 (EE) at 100 mA cm^{-2}	8000@ 100 mA cm^{-2} 900@ 200 mA cm^{-2} Cell Stack	65
12.	0.1M $Zn(OH)_4^{2-}$ + 1M OH^-	0.4M $Fe(CN)_6^{4-}$ + 1M OH^-	Montmorillonite-based separator	80 (EE) at 140 mA cm^{-2}	500 @ 140 mA cm−2.	74
13.	0.1M $ZnCl_2$ + 2M NaCl	0.1M $Fe(bpy)_3Cl_2$ + 2M NaCl	Nafion-115	86.19% @ 1 mA cm-2	20 @ 1 mA cm-2	73

View Article Online
DOI: 10.1039/D4YA00358F

Acknowledgments

Dr. M. U. acknowledges the Amrita Vishwa Vidyapeetham "Seed Grant" Project (***Proposal ID: ASG2022069***) for providing financial support.

Conflict of Interest:

The author declares no conflict of interest.

References:

1. Deng, Y.; Wang, Y.; Xing, X.; Xiong, Y.; Xu, S.; Wang, R. Requirement on the Capacity of Energy Storage to Meet the 2 °C Goal *Sustainability* [Online], 2024.
2. Tang, X.; Zhu, C.; Yang, Y.; Qi, S.; Cai, M.; Alodhayb, A. N.; Ma, J., Additive regulating Li+ solvation structure to construct dual LiF−rich electrode electrolyte interphases for sustaining 4.6 V Li||LiCoO2 batteries. *Chinese Chemical Letters* **2024,** *35* (12), 110014.
3. Zhu, C.; Wu, D.; Wang, C.; Ma, J., Flame-Retardant, Self-Purging, High-Voltage Electrolyte for Safe and Long-Cycling Sodium Metal Batteries. *Advanced Functional Materials* **2024,** *n/a* (n/a), 2406764.
4. Wu, D.; Zhu, C.; Wang, H.; Huang, J.; Jiang, G.; Yang, Y.; Yang, G.; Tang, D.; Ma, J., Mechanically and Thermally Stable Cathode Electrolyte Interphase Enables High-temperature, High-voltage Li||LiCoO2 Batteries. *Angewandte Chemie International Edition* **2024,** *63* (7), e202315608.
5. Sánchez-Díez, E.; Ventosa, E.; Guarnieri, M.; Trovò, A.; Flox, C.; Marcilla, R.; Soavi, F.; Mazur, P.; Aranzabe, E.; Ferret, R., Redox flow batteries: Status and perspective towards sustainable stationary energy storage. *Journal of Power Sources* **2021,** *481*, 228804.
6. Arévalo-Cid, P.; Dias, P.; Mendes, A.; Azevedo, J., Redox flow batteries: a new frontier on energy storage. *Sustainable Energy & Fuels* **2021,** *5* (21), 5366-5419.
7. Weber, A. Z.; Mench, M. M.; Meyers, J. P.; Ross, P. N.; Gostick, J. T.; Liu, Q., Redox flow batteries: a review. *Journal of Applied Electrochemistry* **2011,** *41* (10), 1137-1164.
8. Ashok, A.; Kumar, A., A comprehensive review of metal-based redox flow batteries: progress and perspectives. *Green Chemistry Letters and Reviews* **2024,** *17* (1), 2302834.
9. Aluko, A.; Knight, A., A Review on Vanadium Redox Flow Battery Storage Systems for Large-Scale Power Systems Application. *IEEE Access* **2023,** *11*, 13773-13793.
10. Olabi, A. G.; Allam, M. A.; Abdelkareem, M. A.; Deepa, T. D.; Alami, A. H.; Abbas, Q.; Alkhalidi, A.; Sayed, E. T. Redox Flow Batteries: Recent Development in Main Components, Emerging Technologies, Diagnostic Techniques, Large-Scale Applications, and Challenges and Barriers *Batteries* [Online], 2023.
11. Kwabi, D. G.; Ji, Y.; Aziz, M. J., Electrolyte Lifetime in Aqueous Organic Redox Flow Batteries: A Critical Review. *Chemical Reviews* **2020,** *120* (14), 6467-6489.
12. Liu, Y.; Zhang, J.; Lu, S.; Xiang, Y., Polyoxometalate-based electrolyte materials in redox flow batteries: Current trends and emerging opportunities. *Materials Reports: Energy* **2022,** *2* (2), 100094.
13. Ulaganathan, M.; Aravindan, V.; Yan, Q.; Madhavi, S.; Skyllas-Kazacos, M.; Lim, T. M., Recent Advancements in All-Vanadium Redox Flow Batteries. *Advanced Materials Interfaces* **2016,** *3* (1), 1500309.
14. Suresh, S.; Ulaganathan, M.; Venkatesan, N.; Periasamy, P.; Ragupathy, P., High performance zinc-bromine redox flow batteries: Role of various carbon felts and cell configurations. *Journal of Energy Storage* **2018,** *20*, 134-139.

View Article Online
DOI: 10.1039/D4YA00358F

15. Ulaganathan, M.; Suresh, S.; Mariyappan, K.; Periasamy, P.; Pitchai, R., New Zinc–Vanadium (Zn–V) Hybrid Redox Flow Battery: High-Voltage and Energy-Efficient Advanced Energy Storage System. *ACS Sustainable Chemistry & Engineering* **2019,** *7* (6), 6053-6060.
16. Amini, K.; Pritzker, M., Voltage Loss Analysis of Zinc-Cerium Redox Flow Batteries. *ECS Meeting Abstracts* **2020,** *MA2020-02* (45), 3732.
17. Xie, X.; Mushtaq, F.; Wang, Q.; Daoud, W. A., The Renaissance of the Zn-Ce Flow Battery: Dual-Membrane Configuration Enables Unprecedentedly High Efficiency. *ACS Energy Letters* **2022,** *7* (10), 3484-3491.
18. Cao, X.; Wang, S.; Xue, X., A Zn−Ce Redox Flow Battery with Ethaline Deep Eutectic Solvent. *ChemSusChem* **2021,** *14* (7), 1747-1755.
19. Xu, Z.; Fan, Q.; Li, Y.; Wang, J.; Lund, P. D., Review of zinc dendrite formation in zinc bromine redox flow battery. *Renewable and Sustainable Energy Reviews* **2020,** *127*, 109838.
20. Lee, J.-N.; Do, E.; Kim, Y.; Yu, J.-S.; Kim, K. J., Development of titanium 3D mesh interlayer for enhancing the electrochemical performance of zinc–bromine flow battery. *Scientific Reports* **2021,** *11* (1), 4508.
21. Wang, Y.; Niu, Z.; Zheng, Q.; Zhang, C.; Ye, J.; Dai, G.; Zhao, Y.; Zhang, X., Zn-based eutectic mixture as anolyte for hybrid redox flow batteries. *Scientific Reports* **2018,** *8* (1), 5740.
22. Park, J.; Kim, M.; Choi, J.; Lee, S.; Kim, J.; Han, D.; Jang, H.; Park, M., Recent Progress in High-voltage Aqueous Zinc-based Hybrid Redox Flow Batteries. *Chemistry – An Asian Journal* **2023,** *18* (2), e202201052.
23. Zhao, Q.-Y.; Yin, G.-Y.; Liu, Y.-F.; Tang, R.-R.; Wu, X.-W.; Zeng, X.-X., Recent advances in material chemistry for zinc enabled redox flow batteries. *Carbon Neutralization* **2023,** *2* (1), 90-114.
24. Chen, N.; Wang, W.; Ma, Y.; Chuai, M.; Zheng, X.; Wang, M.; Xu, Y.; Yuan, Y.; Sun, J.; Li, K.; Meng, Y.; Shen, C.; Chen, W., Aqueous Zinc–Chlorine Battery Modulated by a MnO2 Redox Adsorbent. *Small Methods* **2023,** *n/a* (n/a), 2201553.
25. Pei, Z.; Zhu, Z.; Sun, D.; Cai, J.; Mosallanezhad, A.; Chen, M.; Wang, G., Review of the I−/I3− redox chemistry in Zn-iodine redox flow batteries. *Materials Research Bulletin* **2021,** *141*, 111347.
26. Zhang, H.; Sun, C.; Ge, M. Review of the Research Status of Cost-Effective Zinc–Iron Redox Flow Batteries *Batteries* [Online], 2022.
27. Naresh, R. p.; Mariyappan, K.; Dixon, D.; Ulaganathan, M.; Ragupathy, P., Investigations on New Electrolyte Composition and Modified Membrane for High Voltage Zinc−Manganese Hybrid Redox Flow Batteries. *Batteries & Supercaps* **2021,** *4* (9), 1464-1472.
28. Naresh, R.; Pol, V. G.; Ragupathy, P., Energy storage mechanism, advancement, challenges, and perspectives on vivid manganese redox couples. *Energy Advances* **2023,** *2* (7), 948-964.
29. Wu, X.; Markir, A.; Xu, Y.; Zhang, C.; Leonard, D. P.; Shin, W.; Ji, X., A Rechargeable Battery with an Iron Metal Anode. *Advanced Functional Materials* **2019,** *29* (20), 1900911.
30. Tucker, M. C.; Lambelet, D.; Oueslati, M.; Williams, B.; Wang, W.-C. J.; Weber, A. Z., Improved low-cost, non-hazardous, all-iron cell for the developing world. *Journal of Power Sources* **2016,** *332*, 111-117.
31. Qiu, R.; Zheng, J. Y.; Cha, H. G.; Jung, M. H.; Lee, K. J.; Kang, Y. S., One-dimensional ferromagnetic dendritic iron wire array growth by facile electrochemical deposition. *Nanoscale* **2012,** *4* (5), 1565-1567.
32. Deshmukh, S.; Thamizhselvan, R.; Mariyappan, K.; Kathiresan, M.; Ulaganathan, M.; Ragupathy, P., Hybrid Aqueous Alkaline Zinc/TEMPO Flow Battery: A Sustainable High Voltage Green Energy Storage Device. *Journal of The Electrochemical Society* **2023,** *170* (5), 050522.
33. Thamizhselvan, R.; Naresh, R.; Sekar, R.; Ulaganathan, M.; Pol, V. G.; Ragupathy, P., Redox flow batteries: Pushing the cell voltage limits for sustainable energy storage. *Journal of Energy Storage* **2023,** *61*, 106622.
34. Armstrong, R. D.; Baurhoo, I., The dissolution of iron in concentrated alkali. *Journal of Electroanalytical Chemistry and Interfacial Electrochemistry* **1972,** *40* (2), 325-338.

35. Hawthorne, K. L.; Wainright, J. S.; Savinell, R. F., Studies of Iron-Ligand Complexes for an All-Iron Flow Battery Application. *Journal of The Electrochemical Society* **2014,** *161* (10), A1662.
36. Chen, Y. W. D.; Santhanam, K. S. V.; Bard, A. J., Solution Redox Couples for Electrochemical Energy Storage: I . Iron (III)-Iron (II) Complexes with O-Phenanthroline and Related Ligands. *Journal of The Electrochemical Society* **1981,** *128* (7), 1460.
37. Wen, Y. H.; Zhang, H. M.; Qian, P.; Zhou, H. T.; Zhao, P.; Yi, B. L.; Yang, Y. S., A study of the Fe(III)/Fe(II)–triethanolamine complex redox couple for redox flow battery application. *Electrochimica Acta* **2006,** *51* (18), 3769-3775.
38. Murthy, A. S. N.; Srivastava, T., Fe(III)/Fe(II) — ligand systems for use as negative half-cells in redox-flow cells. *Journal of Power Sources* **1989,** *27* (2), 119-126.
39. Hu, J.; Yuan, C.; Zhi, L.; Zhang, H.; Yuan, Z.; Li, X., In Situ Defect-Free Vertically Aligned Layered Double Hydroxide Composite Membrane for High Areal Capacity and Long-Cycle Zinc-Based Flow Battery. *Advanced Functional Materials* **2021,** *31* (31), 2102167.
40. Yuan, Z.; Duan, Y.; Liu, T.; Zhang, H.; Li, X., Toward a Low-Cost Alkaline Zinc-Iron Flow Battery with a Polybenzimidazole Custom Membrane for Stationary Energy Storage. *iScience* **2018,** *3*, 40-49.
41. Lu, W.; Zhang, C.; Zhang, H.; Li, X., Anode for Zinc-Based Batteries: Challenges, Strategies, and Prospects. *ACS Energy Letters* **2021,** *6* (8), 2765-2785.
42. Zhang, Q.; Luan, J.; Tang, Y.; Ji, X.; Wang, H., Interfacial Design of Dendrite-Free Zinc Anodes for Aqueous Zinc-Ion Batteries. *Angewandte Chemie International Edition* **2020,** *59* (32), 13180-13191.
43. Zhang, J.; Jiang, G.; Xu, P.; Ghorbani Kashkooli, A.; Mousavi, M.; Yu, A.; Chen, Z., An all-aqueous redox flow battery with unprecedented energy density. *Energy & Environmental Science* **2018,** *11* (8), 2010-2015.
44. Vetriselvam, Y.; Ramachandran, G. S.; Naresh, R.; Mariyappan, K.; Pitchai, R.; Ulaganathan, M., Improved electro-kinetics of new electrolyte composition for realizing high-performance zinc-bromine redox flow battery. *Next Energy* **2024,** *4*, 100123.
45. Ibanez, J. G.; Choi, C. S.; Becker, R. S., Aqueous Redox Transition Metal Complexes for Electrochemical Applications as a Function of pH. *Journal of The Electrochemical Society* **1987,** *134* (12), 3083.
46. Kingsbury, R. S.; Bruning, K.; Zhu, S.; Flotron, S.; Miller, C. T.; Coronell, O., Influence of Water Uptake, Charge, Manning Parameter, and Contact Angle on Water and Salt Transport in Commercial Ion Exchange Membranes. *Industrial & Engineering Chemistry Research* **2019,** *58* (40), 18663-18674.
47. Liu, X.; Zhang, H.; Duan, Y.; Yuan, Z.; Li, X., Effect of Electrolyte Additives on the Water Transfer Behavior for Alkaline Zinc–Iron Flow Batteries. *ACS Applied Materials & Interfaces* **2020,** *12* (46), 51573-51580.
48. Mariyappan, K.; Saravanakumar, P.; Thamizhselvan, R.; Ragupathy, P.; Ulaganathan, M., In-situ N-rGO Scaffold @3D Graphite Felt for High Power Polyhalide Hybrid Redox Flow Battery. *Advanced Materials Technologies* **2023,** *8* (3), 2200869.
49. Ulaganathan, M.; Mariyappan, K.; Suresh, S.; Ragupathy, P., Graphene Quantum Dot beyond Electrocatalyst: An In Situ Electrolyte Catalyst towards Improved Reaction Kinetics of VO2+/VO2+ Redox Couples. *Journal of The Electrochemical Society* **2020,** *167* (14), 140540.
50. Chen, Z.; Yu, W.; Liu, Y.; Zeng, Y.; He, Q.; Tan, P.; Ni, M., Mathematical modeling and numerical analysis of alkaline zinc-iron flow batteries for energy storage applications. *Chemical Engineering Journal* **2021,** *405*, 126684.
51. Beck, V. A.; Wong, J. J.; Jekel, C. F.; Tortorelli, D. A.; Baker, S. E.; Duoss, E. B.; Worsley, M. A., Computational design of microarchitected porous electrodes for redox flow batteries. *Journal of Power Sources* **2021,** *512*, 230453.
52. Arora, P.; Zhang, Z., Battery Separators. *Chemical Reviews* **2004,** *104* (10), 4419-4462.
53. Park, M.; Ryu, J.; Wang, W.; Cho, J., Material design and engineering of next-generation flow-battery technologies. *Nature Reviews Materials* **2016,** *2* (1), 16080.

54. Gong, K.; Ma, X.; Conforti, K. M.; Kuttler, K. J.; Grunewald, J. B.; Yeager, K. L.; Bazant, M. Z.; Gu, S.; Yan, Y., A zinc–iron redox-flow battery under $100 per kW h of system capital cost. *Energy & Environmental Science* **2015,** *8* (10), 2941-2945.
55. Lin, K.; Gómez-Bombarelli, R.; Beh, E. S.; Tong, L.; Chen, Q.; Valle, A.; Aspuru-Guzik, A.; Aziz, M. J.; Gordon, R. G., A redox-flow battery with an alloxazine-based organic electrolyte. *Nature Energy* **2016,** *1* (9), 16102.
56. Chu, S.; Cui, Y.; Liu, N., The path towards sustainable energy. *Nature Materials* **2017,** *16* (1), 16-22.
57. Liu, T.; Wei, X.; Nie, Z.; Sprenkle, V.; Wang, W., A Total Organic Aqueous Redox Flow Battery Employing a Low Cost and Sustainable Methyl Viologen Anolyte and 4-HO-TEMPO Catholyte. *Advanced Energy Materials* **2016,** *6* (3), 1501449.
58. Zhou, X. L.; Zhao, T. S.; An, L.; Wei, L.; Zhang, C., The use of polybenzimidazole membranes in vanadium redox flow batteries leading to increased coulombic efficiency and cycling performance. *Electrochimica Acta* **2015,** *153*, 492-498.
59. Yuan, Z.; Duan, Y.; Zhang, H.; Li, X.; Zhang, H.; Vankelecom, I., Advanced porous membranes with ultra-high selectivity and stability for vanadium flow batteries. *Energy & Environmental Science* **2016,** *9* (2), 441-447.
60. Chen, Y.; Xiong, P.; Xiao, S.; Zhu, Y.; Peng, S.; He, G., Ion conductive mechanisms and redox flow battery applications of polybenzimidazole-based membranes. *Energy Storage Materials* **2022,** *45*, 595-617.
61. Selverston, S.; Savinell, R. F.; Wainright, J. S., Zinc-Iron Flow Batteries with Common Electrolyte. *Journal of The Electrochemical Society* **2017,** *164* (6), A1069.
62. Yuan, Z.; Liu, X.; Xu, W.; Duan, Y.; Zhang, H.; Li, X., Negatively charged nanoporous membrane for a dendrite-free alkaline zinc-based flow battery with long cycle life. *Nature Communications* **2018,** *9* (1), 3731.
63. Chang, S.; Ye, J.; Zhou, W.; Wu, C.; Ding, M.; Long, Y.; Cheng, Y.; Jia, C., A low-cost SPEEK-K type membrane for neutral aqueous zinc-iron redox flow battery. *Surface and Coatings Technology* **2019,** *358*, 190-194.
64. Yang, M.; Xu, Z.; Xiang, W.; Xu, H.; Ding, M.; Li, L.; Tang, A.; Gao, R.; Zhou, G.; Jia, C., High performance and long cycle life neutral zinc-iron flow batteries enabled by zinc-bromide complexation. *Energy Storage Materials* **2022,** *44*, 433-440.
65. Wang, G.; Zou, H.; Xu, Z.; Tang, A.; Zhong, F.; Zhu, X.; Qin, C.; Ding, M.; You, W.; Jia, C., Unlocking the solubility limit of ferrocyanide for high energy density redox flow batteries. *Materials Today Energy* **2022,** *28*, 101061.
66. Kim, Y.; Yun, D.; Jeon, J., Performance improvement of aqueous zinc-iron flow batteries through organic ligand complexation of Fe(II)/Fe(III). *Electrochimica Acta* **2020,** *354*, 136691.
67. Jeena, C. B.; Elsa, P. J.; Moly, P. P.; Ambily, K. J.; Joy, V. T., A dendrite free Zn-Fe hybrid redox flow battery for renewable energy storage. *Energy Storage* **2022,** *4* (1), e275.
68. Lee, B.-S.; Cui, S.; Xing, X.; Liu, H.; Yue, X.; Petrova, V.; Lim, H.-D.; Chen, R.; Liu, P., Dendrite Suppression Membranes for Rechargeable Zinc Batteries. *ACS Applied Materials & Interfaces* **2018,** *10* (45), 38928-38935.
69. Hao, X.; Hu, J.; Zhang, Z.; Luo, Y.; Hou, H.; Zou, G.; Ji, X., Interfacial regulation of dendrite-free zinc anodes through a dynamic hydrophobic molecular membrane. *Journal of Materials Chemistry A* **2021,** *9* (25), 14265-14269.
70. Yang, J.; Yan, H.; Hao, H.; Song, Y.; Li, Y.; Liu, Q.; Tang, A., Synergetic Modulation on Solvation Structure and Electrode Interface Enables a Highly Reversible Zinc Anode for Zinc–Iron Flow Batteries. *ACS Energy Letters* **2022,** *7* (7), 2331-2339.
71. Zhang, Y.; Henkensmeier, D.; Kim, S.; Hempelmann, R.; Chen, R., Enhanced reaction kinetics of an aqueous Zn–Fe hybrid flow battery by optimizing the supporting electrolytes. *Journal of Energy Storage* **2019,** *25*, 100883.

72. Chen, D.; Kang, C.; Duan, W.; Yuan, Z.; Li, X., A non-ionic membrane with high performance for alkaline zinc-iron flow battery. *Journal of Membrane Science* **2021,** *618*, 118585.
73. Xie, Z.; Wei, L.; Zhong, S., An aqueous ZnCl2/Fe(bpy)3Cl2 flow battery with mild electrolyte. *Frontiers of Materials Science* **2020,** *14* (4), 442-449.
74. Chen, H.; Kang, C.; Shang, E.; Liu, G.; Chen, D.; Yuan, Z., Montmorillonite-Based Separator Enables a Long-Life Alkaline Zinc–Iron Flow Battery. *Industrial & Engineering Chemistry Research* **2023,** *62* (1), 676-684.
75. Chen, Z.; Liu, Y.; Yu, W.; He, Q.; Ni, M.; Yang, S.; Zhang, S.; Tan, P., Cost evaluation and sensitivity analysis of the alkaline zinc-iron flow battery system for large-scale energy storage applications. *Journal of Energy Storage* **2021,** *44*, 103327.
76. Xie, C.; Duan, Y.; Xu, W.; Zhang, H.; Li, X., A Low-Cost Neutral Zinc–Iron Flow Battery with High Energy Density for Stationary Energy Storage. *Angewandte Chemie International Edition* **2017,** *56* (47), 14953-14957.

View Article Online
DOI: 10.1039/D4YA00358F

Data availability statement

There is no data used in this review article.